

E14-2011-17

N. Ya. Tsibakhashvili^{1,2}, E. I. Kirkesali¹, D. T. Pataraya³,
M. A. Gurielidze³, T. L. Kalabegishvili^{1,2}, D. N. Gvarjaladze²,
G. I. Tsertsvadze⁴, M. V. Frontasyeva⁵, I. I. Zinicovskaia⁵,
M. S. Wakstein⁶, S. N. Khakhanov⁷, N. V. Shvindina⁷,
V. Ya. Shklover⁷

MICROBIAL SYNTHESIS OF SILVER
NANOPARTICLES BY *STREPTOMYCES GLAUCUS*
AND *SPIRULINA PLATENSIS*

Submitted to «Advanced Science Letters»

¹Andronikashvili Institute of Physics, Tbilisi, Georgia

²Ilia State University, Tbilisi, Georgia

³Durmishidze Institute of Biochemistry and Biotechnology, Tbilisi, Georgia

⁴Georgian Technical University, Tbilisi, Georgia

⁵Joint Institute for Nuclear Research, Dubna, Russia

⁶ Scientific and Technological Research Centre «Nanotech-Dubna», Dubna, Russia

⁷Systems for Microscopy and Analysis, Application Laboratory Department, Moscow, Russia

Цибакхашвили Н. Я. и др.

E14-2011-17

Синтез наночастиц серебра микроорганизмами *Streptomyces glaucus* и *Spirulina platensis*

Впервые в Грузии для синтеза наночастиц серебра использовался вид актиномицетов *Streptomyces glaucus* 71 MD, выделенный из соевой ризосферы. Снимки наночастиц, полученные на просвечивающем электронном микроскопе (ПЭМ), показывают, что большая часть частиц, синтезированных этими микроорганизмами из AgNO_3 , имела сферическую форму со средним размером 13 нм. Снимки растрового электронного микроскопа (РЭМ) подтверждают внеклеточный синтез наночастиц, что дает преимущества с точки зрения их применения. Образование наночастиц протекает вне клеток и с участием другого микроорганизма — сине-зеленой микроводоросли *Spirulina platensis*. При этом синтез наночастиц зависит не только от начальной концентрации AgNO_3 , но и от времени взаимодействия.

Работа выполнена в Лаборатории нейтронной физики им. И. М. Франка ОИЯИ, в Институте физики им. Э. Л. Андроникашвили АН Грузии (Тбилиси) и в Государственном университете им. И. Чавчавадзе, Тбилиси (Грузия).

Препринт Объединенного института ядерных исследований. Дубна, 2011

Tsibakhashvili N. Ya. et al.

E14-2011-17

Microbial Synthesis of Silver Nanoparticles by *Streptomyces glaucus* and *Spirulina platensis*

For the first time in Georgia a novel actinomycete strain *Streptomyces glaucus* 71 MD isolated from a soy rhizosphere has been used for microbial synthesis of silver nanoparticles. The Transmission Electron Microscope (TEM) images revealed that most of the particles produced by these microorganisms from AgNO_3 are spherical-like in shape with an average size of 13 nm. The Scanning Electron Microscope (SEM) allowed one to observe extracellular synthesis of nanoparticles, which has many advantages from the point of view of applications. Production of silver nanoparticles proceeds extracellularly with the participation of another microorganism, blue-green microalgae *Spirulina platensis*. It is shown that the production rate of the nanoparticles depends not only on the initial concentration of AgNO_3 but also varies with time in a non-monotonic way.

The investigation has been performed at the Frank Laboratory of Neutron Physics, JINR, at the Andronikashvili Institute of Physics of the Georgian Academy of Sciences, Tbilisi and at the Ilia State University, Tbilisi (Georgia).

Preprint of the Joint Institute for Nuclear Research. Dubna, 2011

INTRODUCTION

Silver nanoparticles have a great number of applications, e.g., in nonlinear optics, spectrally selective coating for solar energy absorption, biolabelling, intercalation materials for electrical batteries, high-sensitivity biomolecular detection and diagnostics, antimicrobials and therapeutics, catalysis and microelectronics [1–3]. Now silver nanoparticles are commonly synthesized on chemical/physical pathways, which are low-yield, energy-intensive, difficult to scale up, often producing high levels of hazardous wastes, and may require the use of costly organometallic precursors. So, these techniques yield extremely expensive materials. In addition, these aqua-chemical routes lead to particles with a strong hydrophobic surface, requiring further special modification in order to overcome the resulting problems for application. Also, the produced nanoparticles exhibit undesirable aggregation with time. Hence, there is an ever-growing need to develop inexpensive, clean, nontoxic, and environmentally safe synthesis procedures. Biological methods, if properly designed and implemented, make it all possible [4].

In the last years great attention has been paid to microbial technologies of nanoparticle production [5,6]. Microbial cells have developed specific mechanisms for interacting with inorganic ions in the aqueous environment. Sometimes these microbial processes result in inorganic precipitation, both intracellular and extracellular [7].

Various microorganisms (bacteria, yeast, fungi) are known to synthesize silver nanoparticles [5,6,8–12]. The produced nanoparticles have different size and shape. Nanoparticles resulting from some microbial processes are composite materials and consist of inorganic component and special organic matrix (proteins, lipids, or polysaccharides) and they have unique chemical and physical properties different from the properties of conventionally produced nanoparticles and of other microorganisms even when they are incubated in the same medium under the same conditions. So, it is important to examine new classes of microbes to synthesize silver nanoparticles with technologically important properties.

It is also important that the methods of chemical synthesis may entail the presence of some toxic chemical species adsorbed on the surface that could have adverse effects in medical applications. Synthesis of nanoparticles using microorganisms can potentially eliminate this problem by making the nanoparticles more

biocompatible. However, up to date, most of the microorganisms that have been reportedly used for synthesis of silver nanoparticles are pathogenic to either plants and/or humans [5, 12]. So, last years the researchers have turned to nonpathogenic microorganisms [13, 14]. *Spirulina platensis*, a blue-green microalgae (cyanobacteria), is an important representative among these microorganisms. Moreover, it is used as a biologically active food additive for humans and animals [15]. Although the therapeutic potential of *S. platensis* is promising, its property of bioreduction of inorganic materials is yet to be exploited. Recently, the first study of this subject has appeared [12]. However, as the microbial synthesis of nanoparticles strongly depends on the experimental conditions, further investigations are necessary.

In this study, we aimed at testing the ability of *Streptomyces glaucus* 71 MD, a novel strain of actinomycetes isolated in Georgia, to produce silver nanoparticles. The authors have great experience in studying heavy metal interactions with *S. platensis* [16, 17]. In addition, synthesis of silver nanoparticles by *S. platensis* was investigated in more detail. The Scanning Electron Microscope (SEM) and the Transmission Electron Microscope (TEM) were used as the key techniques.

Actinomycetes-mediated «green chemistry» approach to the synthesis of nanoparticles has many advantages [18]. Specifically, compared to bacteria, fungi and actinomycetes are known to secrete much higher amounts of proteins, thereby significantly increasing the productivity of this biosynthetic approach. In addition, actinomycetes are classified as prokaryotes and can be manipulated genetically without much difficulty in the future in order to achieve better control over size and polydispersity of the nanoparticles.

EXPERIMENTAL

Isolation and Characterization of the Actinomycetes Strain *Streptomyces glaucus* 71 MD. The strain was isolated from the soy rhizosphere using the method of dilution [19, 20]. Incubation was carried out in a thermostat at 26–28 °C for 14 days. Pure colonies were subjected to various biochemical tests to investigate into their morphological and physiological characteristics. Growth ability of the culture was studied in different synthetic and organic nutrient media. Pridham's method was used to study the carbon source uptake ability [21]. One percent of the carbon source, in particular, monosaccharides (glucose, fructose, galactose, arabinose, xylose, ramnose), alcohols (mannitol, sorbitol, inositol, dulcitol, glycerol), disaccharides (saccharose, lactose, maltose), polysaccharides (starch), and organic acids (sodium citrate, sodium lactate, and sodium succinate), was added to nutrient medium. Fedorov's nutrient medium was used to establish the uptake of different sources of nitrogen [20]. Nitrogen-containing organic and inorganic compounds were used as the nitrogen source. Ability

of actinomycetes to grow on hydrocarbons, such as hexane, benzene, naphthalene, benzopyrene, dichlorobenzene, crude oil containing nutrient medium, was investigated. Hydrocarbon absorption ability of actinomyces was determined according to its growth intensity. Antagonistic properties were studied by the agar block method [22]. *Staphilococcus aureus*, *Echerichia coli*, *Pseudomonas aeruginosa*, *Azospirillum brassilens* G-3, *Mycobacterium phlei*, *Rodococcus spp.*, *Saccharomyces cerevisiae*, *Candida utilis*, *Rhizoctonia spp.*, and *Fusarium solani* strains were selected as the test cultures. Protease activity was determined by Anson's method modified by Petrova [23]. Identification of actinomycetes was performed according to Krassilnikov and Bergey's Manuals [24, 25].

Cultivation of *Streptomyces glaucus* 71 MD. Cells were grown aerobically at pH 7–8, 28–30 °C in 500-ml Erlenmayer flasks. The cells were grown in a liquid medium Gauze-1 [19]: K₂HPO₄ (0.05%), MgSO₄ (0.05%), NaCl (0.05%), KNO₃ (0.1%), FeSO₄×7H₂O (0.001%), starch (2%), yeast extract (0.03%), pH 7.5. The culture was grown with continuous shaking on a shaker (200 rpm) at 30 °C for 9 days. After cultivation, mycelia (cells) were separated from the culture broth by centrifugation (4500 rpm) for 20 min and then the mycelia were washed thrice with sterile distilled water under sterile conditions. The harvested mycelial mass (16 g of wet mycelia) was then resuspended in 100 ml of 10⁻³ M aqueous AgNO₃ solution in 500-ml Erlenmeyer flasks. The whole mixture was put into a shaker at 30 °C (200 rpm).

Cultivation of *S. platensis*. Cells were cultivated in Zarrouk growth media at constant shaking at 30–31 °C, pH 9 [14]. The bacterial cells were harvested after 5–6 days and then were washed twice in distilled water. Then 1 g of wet biomass was placed in a 250-ml Erlenmeyer flask with 100 ml 10⁻³ M aqueous AgNO₃ and incubated at room temperature for different time intervals (1–5 days). The pH was checked during the course of reaction and it was found to be 5.6.

For UV-Vis spectral analysis, a 2-ml sample was taken after different time intervals (1 and 5 days) and the absorbance was measured.

For SEM and X-ray analysis, the bacterial cells were harvested by centrifugation at 12000 g for 20 min and this wet biomass was placed in an adsorption-condensation lyophilizer and dried following the procedure reported in [26].

All chemicals were of ACS-reagent grade and purchased from Sigma (St. Louis, MO, USA).

METHODS

UV-Vis Spectrometry. The UV-Vis spectra of the samples were recorded on a «Cintra 10e» spectrophotometer (GBC Scientific Equipment Pty Ltd. Australia, wave length range of 190–1100 nm).

X-ray Diffraction (XRD). XRD measurements of the bacterial biomass were made on a Dron-2.0 diffractometer. The BCV-23 X-ray tube with the Cu anode

(CuK α radiation, $\lambda = 1.54178 \text{ \AA}$) was used as a source of irradiation; the Ni grid with the width of $20 \mu\text{m}$ was used for filtration of irradiation; the rate of the detector was $2^\circ/\text{min}$, the interval of intensity was 1000 pulses/min and the time constant was 5 s.

Transmission Electron Microscope (TEM). TEM was performed using the Jeol SX-100 equipment (Japan) operating at 100 kV. The TEM studies were done at 50 000x magnification. Samples were prepared by placing a drop of solution of silver nanoparticles on carbon-coated TEM grids. The films on the TEM grids were allowed to dry at room temperature before analysis.

Scanning Electron Microscope. SEM was carried out using the SDB (small dual-beam) FEI Quanta 3D FEG with the EDAX Genesis EDX system with the resolution 1.2 nm. Operational features of the microscope used in the experiment: magnification 5000–150000x; voltage 1–30 kV.

EDAX (Energy-Dispersive Analysis of X-rays). Microprobe analysis of nanoparticle clusters (silver) was conducted with the energy-dispersive X-ray spectrometer (EDAX, USA). The acquisition time ranged from 60 to 100 s, and the accelerating voltage was 20 kV.

RESULTS AND DISCUSSION

The work consisted of two parts: synthesis of silver nanoparticles (i) by *Streptomyces glaucus* 71 MD and (ii) by *S. platensis*.

i) Synthesis of Silver Nanoparticles by a Novel Actinomycetes Strain *Streptomyces glaucus* 71 MD.

Characteristics of a Novel Actinomycete Strain. The strain isolated from a soy rhizosphere showed typical characteristics of *Streptomyces glaucus*. Specifically, it is aerobic and creates a spirally twisted sporophore. The spore envelope is smooth, and the aerial mycelium is bluish-green. It develops melanoid pigments. In a synthetic nutrient medium the growth is good, colonies and the nutrient medium are colorless, the aerial mycelium is bluish-green. In an organic nutrient medium the growth is also good, colonies and the nutrient medium are colorless, and the aerial mycelium is weakly developed, light blue.

From carbohydrate sources the strain intensively uptakes starch, dulcitol, and mannitol and weakly uptakes glucose, lactose, and sodium citrate. It does not uptake fructose and xylose, galactose, maltose, glycerol, sodium lactate, cellulose.

From nitrogen sources it uptakes KNO₃, Ca(NO₃)₂, peptone, leucine, asparagine, β -alanine glycine, asparagine. Antagonistic properties are not well expressed. It does not affect gram-positive and gram-negative bacteria. It inhibits some species of fungi. The culture is mesophilic. SEM images show that the cells of the strain form oval-shaped colonies (Fig. 1). Discrete lipopolysaccharide layers on the bacteria cell surface caused the bacteria to glue to each other.

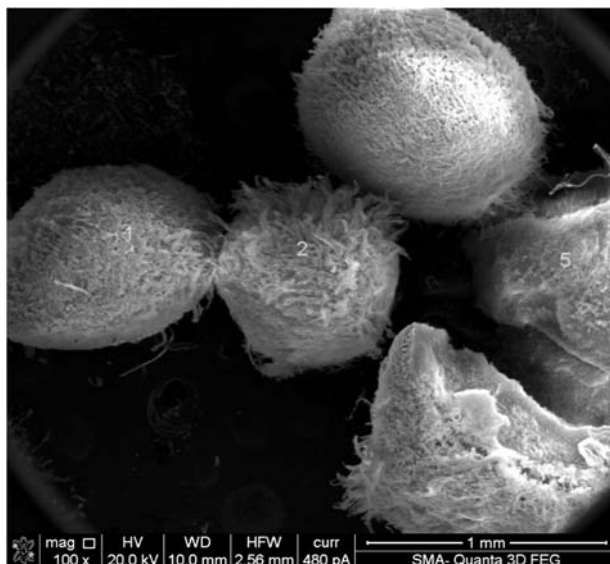


Fig. 1. SEM of the colonies of *Streptomyces glaucus* 71 MD cells

Synthesis of Silver Nanoparticles by *Streptomyces glaucus* 71 MD and Their Characterization. Addition of actinomycetes biomass to a silver nitrate solution led to the appearance of yellowish brown color in the solution after a few days, indicating formation of silver nanoparticles. First, the UV-visible spectroscopy method was used to quantify this process (Fig.2). The spectrum presented in Fig.2 exhibits an absorption peak at 425 nm, which is characteristic of silver nanoparticles [27]. In the case of the silver nitrate solution alone, or actinomycetes cells alone, no change in color was observed for 10 days. Thus, *Streptomyces glaucus* 71 MD could synthesize silver nanoparticles by incubating with a AgNO_3 solution.

Then the cells of *Streptomyces glaucus* 71 MD were imaged by the SEM method after the reaction with the silver nitrate solution for one week. The SEM images (Fig. 3) illustrate that most of the particles are spherical-like and do not create big agglomerates.

In Fig.1 the colonies of the actinomycete cells are numbered. The image with index 3 belongs to a disintegrated colony. The SEM images of the inner area of this colony (Fig.4, *a, b, c*) demonstrate that silver nanoparticles are not observed there, while they exist on the outer surface of the colony (Fig.4, *d*). It seems that the disintegration took place in the process of drying after an exposure to silver salts.

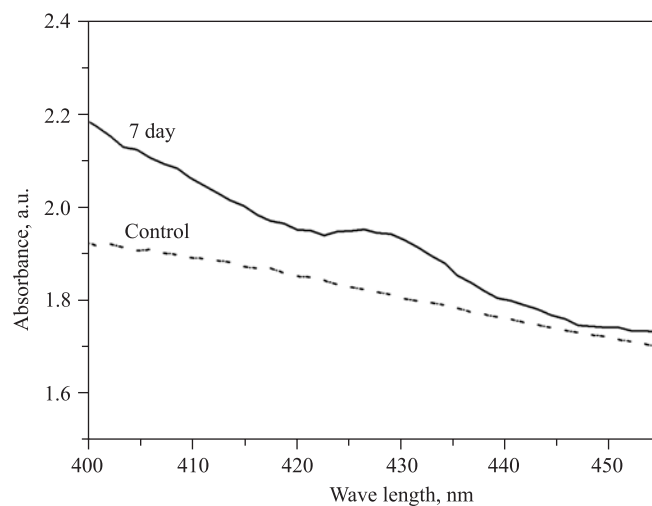


Fig. 2. UV-Vis spectra recorded after one week for the reaction mixture prepared using 1 mM silver nitrate and 1 g biomass of *Streptomyces glaucus* 71 MD

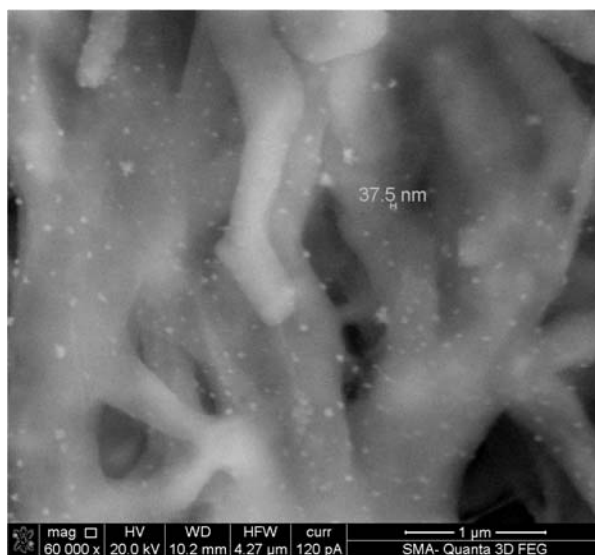


Fig. 3. SEM of *Streptomyces glaucus* 71 MD cells with silver nanoparticles

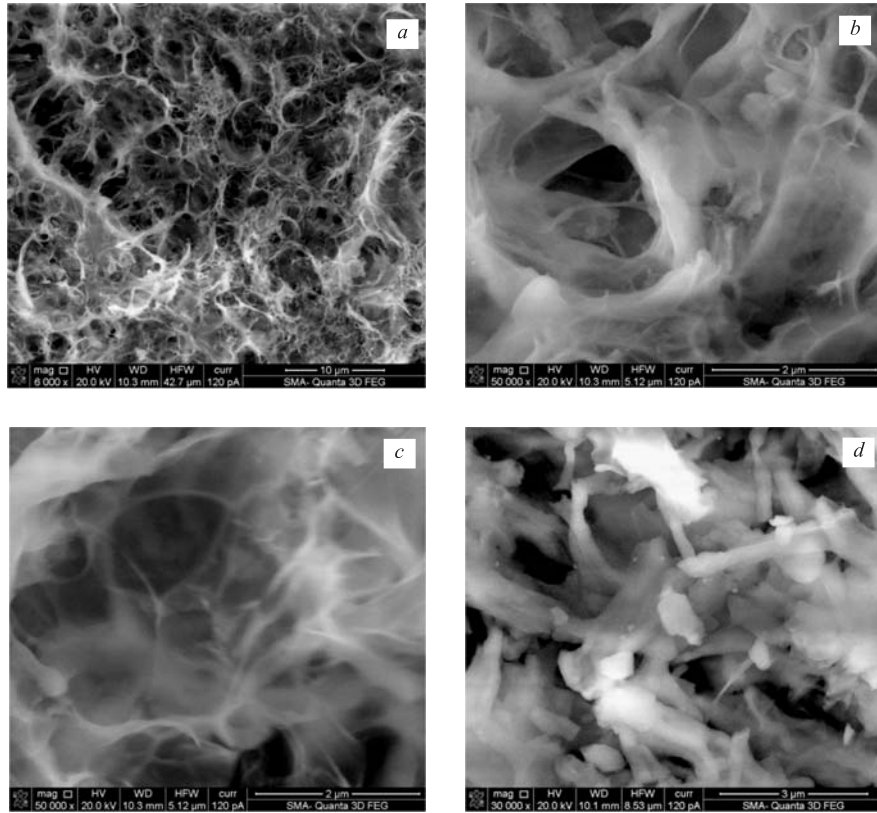


Fig. 4. SEM of *Streptomyces glaucus* 71 MD colony N3: a, b, c) inner area, d) outer surface

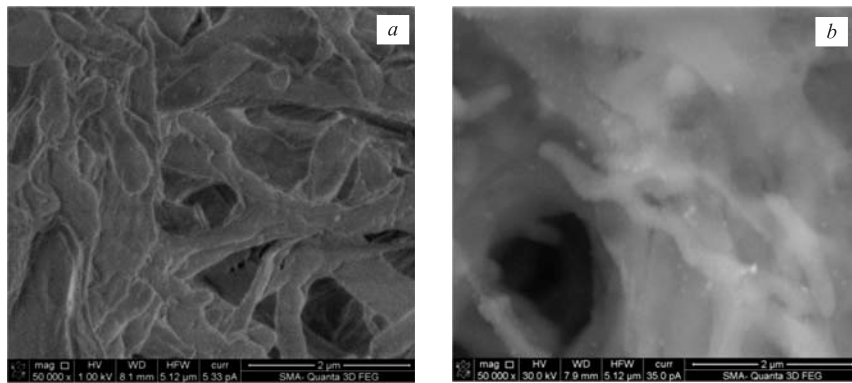
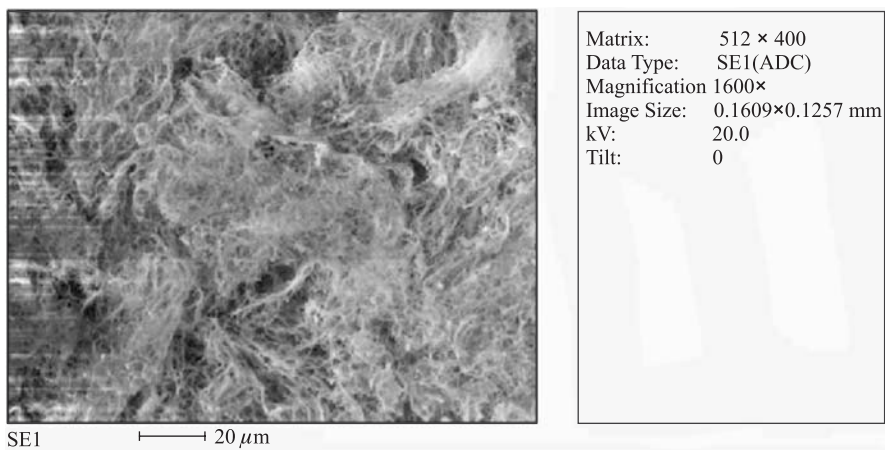


Fig. 5. SEM of *Streptomyces glaucus* 71 MD cell N3 taken at different voltages of accelerating field; a) 1 kV, b) 20 kV



SE1 20 μm

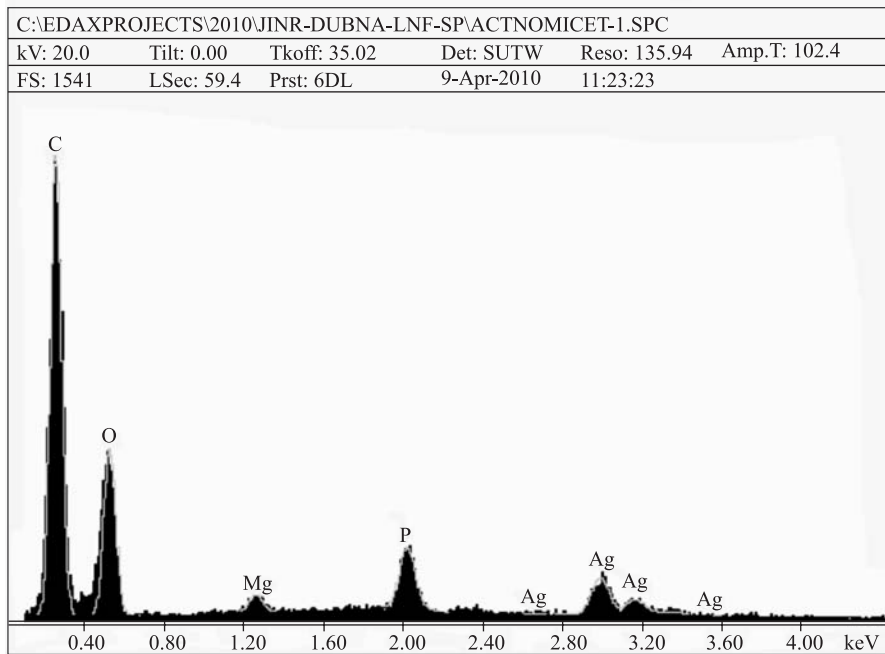


Fig. 6. EDAX spectrum recorded from *Streptomyces glaucus* 71 MD cells after formation of silver nanoparticles. Different X-ray emission peaks are labeled

Figure 5, *a* presents a SEM image of cell taken at the accelerating field voltage of 1 kV. This voltage corresponds to the scanning of the most superficial layer, while, at 30 kV, the electrons penetrate slightly deeper, but it is still a surface,

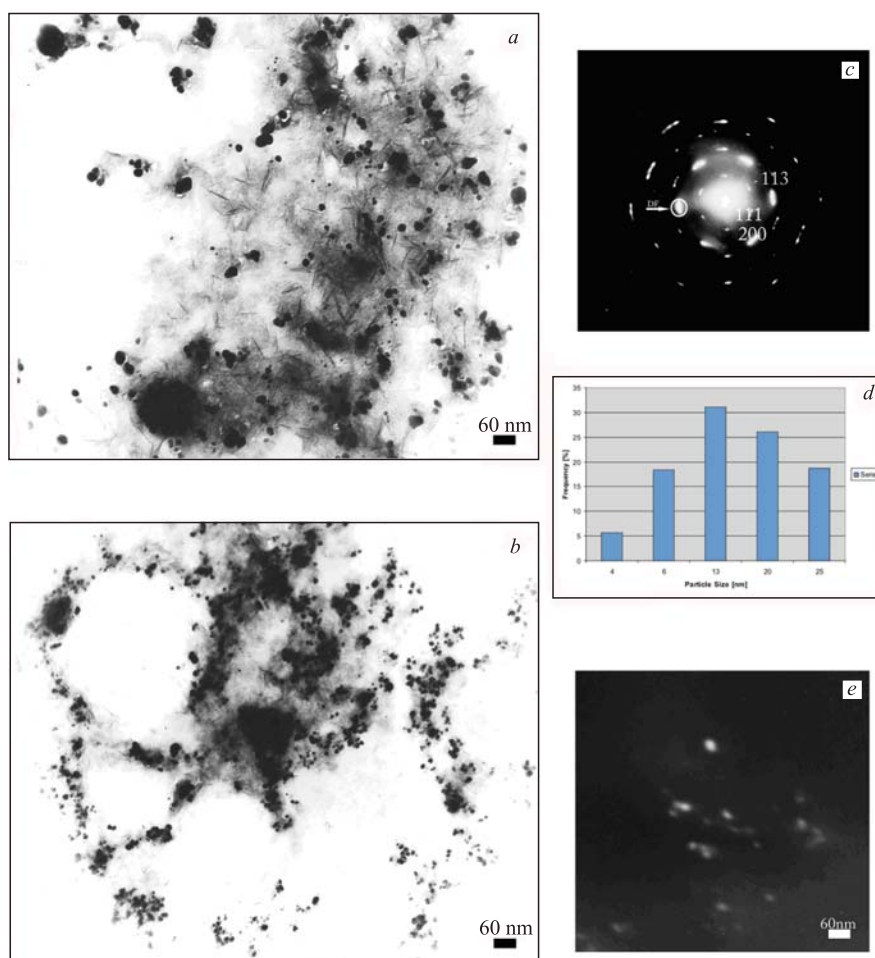


Fig. 7. *a, b*) TEM micrograph recorded from drop-cast films of silver nanoparticle solution formed by the reaction of silver nitrate solution with *Streptomyces glaucus* 71 MD biomass; *c*) selected area diffraction pattern recorded from the silver nanoparticles shown in Fig. 7, *e*; *d*) particle size distribution histogram

and the nanoparticles are attributed to it (Fig. 5, *b*). The SEM results indicate that the process of formation of silver nanoparticles takes place on the surface of the cells. Reduction and surface accumulation of metals may be a process by which microorganisms protect themselves from the toxic effects of metal ions. Today the exact mechanism for formation of silver nanoparticles by microorganisms is not fully understood.

In addition to the images, EDAX (Energy Dispersive Analysis of X-rays) spectra were also registered proving the presence of silver in *Streptomyces glaucus* 71 MD (Fig. 6). The EDAX spectrum was recorded in the spot-profile mode from one of the densely populated silver nanoparticle regions on the surface of the actinomycete cells. All the peaks of Ag are observed and assigned. Signals from C, O, S, P, and Mg atoms were also recorded. The C, O, S, P, and Mg signals are likely to be due to X-ray emission from proteins/enzymes present in the cell wall of the biomass. As is known, proteins can bind to nanoparticles either through free amino groups or cysteine residues in the protein and/or via the electrostatic attraction of negatively charged carboxylate groups in enzymes present in the actinomycetes cell wall of [4].

In the last set of experiments the silver nanoparticles synthesized by *Streptomyces glaucus* 71 MD were characterized using TEM (Fig. 7). Figures 7, *a* and *b* show the TEM images recorded from the drop-coated films of silver nanoparticles synthesized after the reaction of the silver nitrate solution with 2 g of wet *Streptomyces glaucus* 71 MD biomass for 7 days. In Fig. 7, *c* the selected area electron diffraction (SAED) spots that correspond to the [111], [200], [311] planes of the face-centered cubic (fcc) structure of elemental silver [28] are clearly seen. The particle size histogram for the particles shown in this image and in other similar images is given in Fig. 7, *d*. The histogram shows that the particle sizes range from 4 to 25 nm with an average of 13 nm. Comparison of the SEM and TEM images suggests that the tested actinomycetes *Streptomyces glaucus* 71 MD produce relatively monodispersed Ag nanoparticles extracellularly. Extracellular formation of nanoparticles is advantageous over intracellular formation, as it eliminates the need to harvest nanoparticles formed within the cell. In addition, extracellular synthesis of nanoparticles makes it possible to immobilize particles onto the desired solid support for different practical applications.

ii) **Synthesis of Silver Nanoparticles by *S. platensis*.**

In the second part of our work we investigated synthesis of silver nanoparticles by *S. platensis* under different experimental conditions.

As has recently been shown, *S. platensis* produces silver nanoparticles extracellularly in the range of 7–16 nm [12]. Our current experiments have confirmed this result. Figure 8 shows the TEM image recorded from the drop-coated films of silver nanoparticles synthesized after the reaction of the silver nitrate solution with 2 g of wet *S. platensis* biomass for 5 days. Here (Fig. 8, *a*) the SAED patterns that correspond to the [111], [220] planes of the face-centered cubic (fcc) structure of elemental silver are also given. The particle size histogram shows that sizes of silver nanoparticles range from 5 to 20 nm with the average size value of 10 nm (Fig. 8, *c*).

In our further experiments the presence of silver nanoparticles in the biomass of *S. platensis* after exposure to the silver nitrate solution for 1 and 5 days was investigated. For this purpose, the XRD method was first employed (Fig. 9).

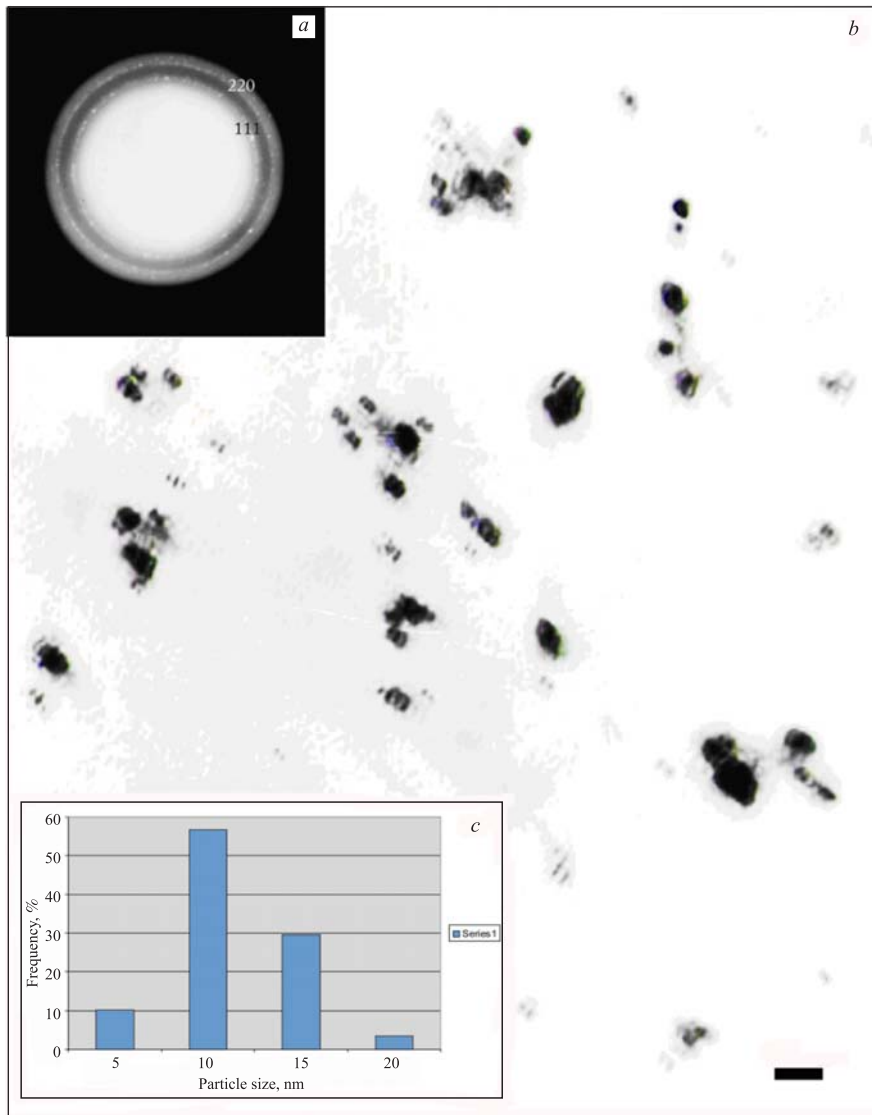


Fig. 8. *a*) Selected area diffraction pattern recorded from the silver nanoparticles; *b*) TEM micrograph recorded from drop-cast films of silver nanoparticle solution formed by the reaction of silver nitrate solution with *S. platensis* biomass; *c*) particle size distribution histogram

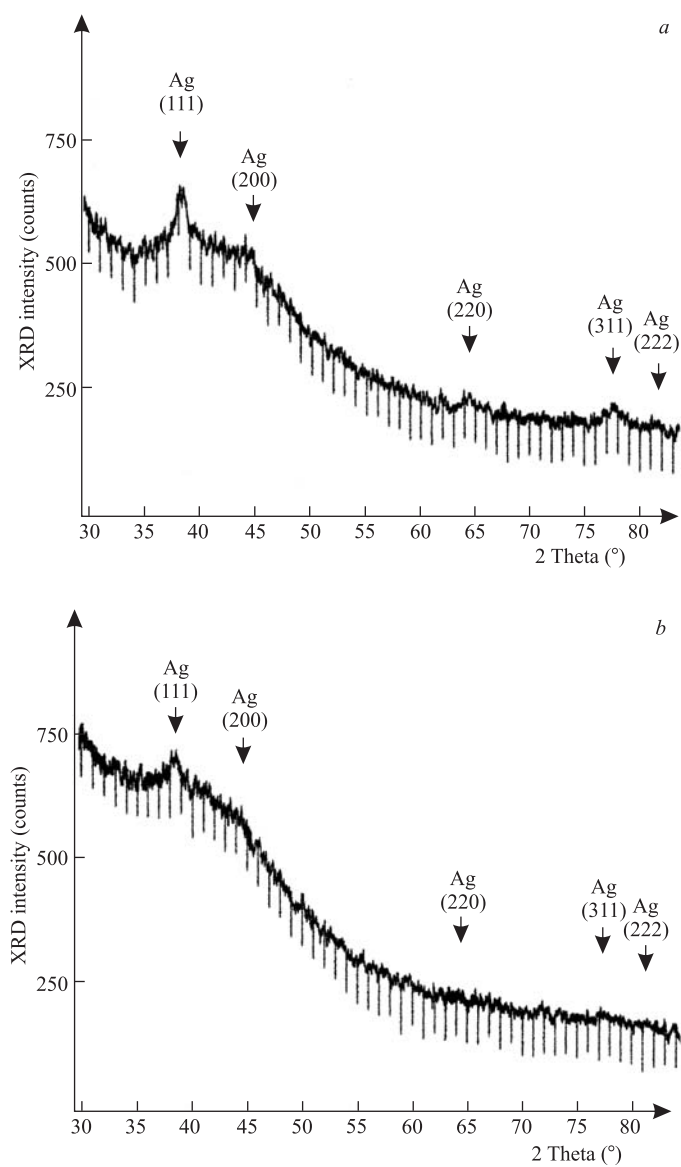
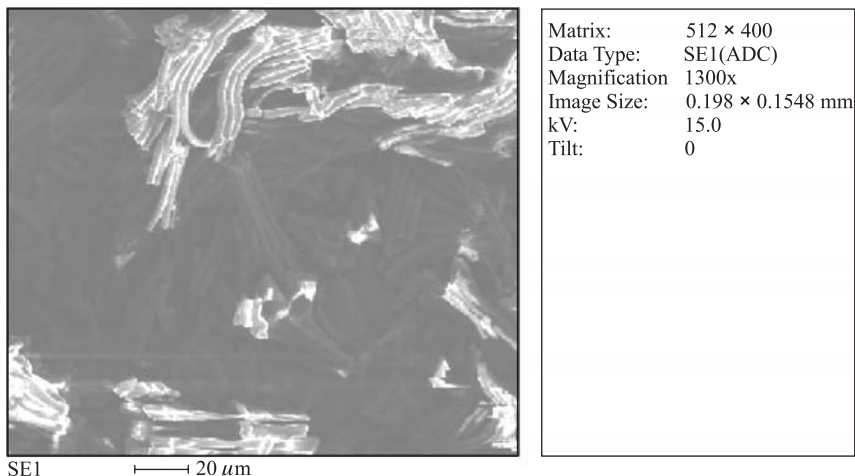


Fig. 9. XRD spectra of silver nanoparticles synthesized using 2 g wet biomass of *S. platen-sis* incubated with 1 mM AgNO₃ for 1 and 5 days



SE1 ← 20 μm

C:\EDAXPROJECTS\2010\JINR-DUBNA-LNF-SP\SPIRULINA-3.SPC					
kV: 15.0	Tilt: 0.00	Tkoff: 35.02	DetSUTW	Reso: 135.94	Amp.T: 102.4
FS: 307	LSec: 285.1	Prst: 300C	9-Apr-2010	11:49:00	

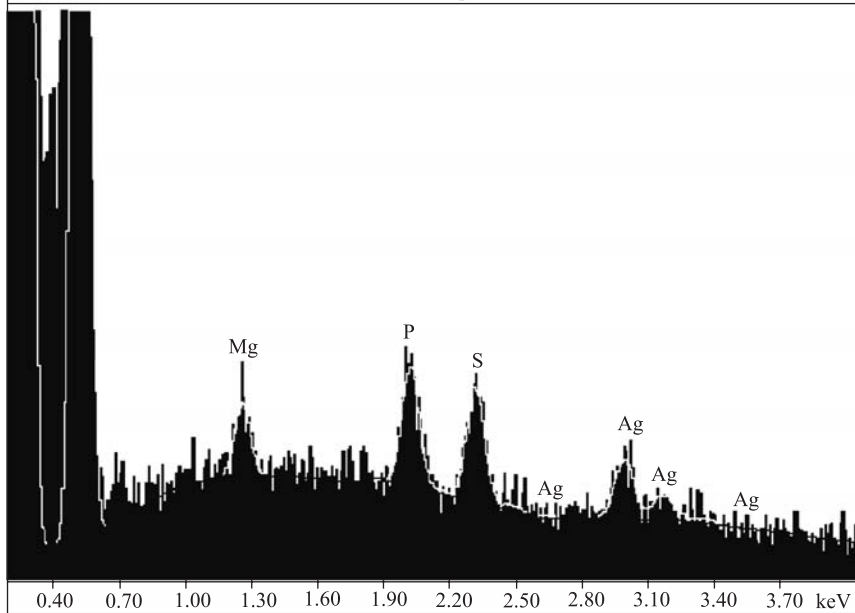


Fig. 10. EDAX spectrum of *S. platensis* cells after exposure to silver nitrate solution. Different X-ray emission peaks are labeled

The diffraction patterns presented in Fig. 9 correspond to the amorphous structure of samples. However, a number of Bragg's reflections corresponding to the fcc structure of silver are also seen here. Specifically, the XRD pattern shows four characteristic peaks corresponding to the (111), (200), (220), (222) and (311) sets of lattice planes. The XRD pattern thus clearly shows that the silver nanoparticles formed by the reduction of Ag^+ ions by *S. platensis* are crystalline in nature. It should be noted that the relative crystalline silver content of the *S. platensis* biomass was not high, not more than 1%, which was at the sensitivity limit of the XRD analysis. This result confirmed that silver nanoparticles were produced in general extracellularly.

EDXA also confirmed the presence of silver nanoparticles in the *S. platensis* biomass (Fig. 10).

Further characterization of silver nanoparticles remained in the cells of *S. platensis* was carried out with SEM (Fig. 11). *S. platensis* is a filamentous cyanobacterium (Fig. 11, *a*). The main morphological feature of this genus is the arrangement of the multicellular cylindrical trichomes in an open left-hand helix along the entire length. The cylindrical trichomes of *S. platensis* were strongly damaged after exposure to 1 mM AgNO_3 for 1 day (Fig. 11, *b*). They became serrated and even broken in many places (Fig. 11, *c*). It is interesting that in cells these visual morphological damages completely disappeared after exposure to the silver nitrate solution for 5 days (Fig. 11, *d*). In addition, the biomass of *S. platensis* increased (from 112 mg after 1 day to 140 mg after 5 days). So, it can be suggested that *S. platensis* cells were adapted to the toxic action of silver in five days.

Figure 12 presents SEM images of *S. platensis* cells with silver nanoparticles and illustrates that on the surface of the cyanobacteria both the size and the distribution of the silver nanoparticles depend on the time of silver action. Specifically, after one day of the silver ion action, large agglomerates of nanoparticles could be observed. The mean size of the nanoparticles observed in these agglomerates is about 27 nm (Fig. 12, *a, b*). However, after immersion of *S. platensis* cells in the silver nitrate solution for 5 days, the produced silver nanoparticles are relatively uniformly distributed along the surface of the cyanobacterium cells. In this case, the maximum size of the formed agglomerates is about 235 nm and the minimum size is 75 nm (Fig. 12, *c, d*).

As is known, the cell growth and metal incubation conditions can be the cause for the formation of particles of different sizes. For example, addition of AgNO_3 to the photoautotrophic cyanobacterium *Plectonema boryanum* caused production of silver nanoparticles both inside and outside the microbial cells [9]. At 60 °C, silver nanoparticles were deposited on the cell surface. At 100 °C, the cyanobacteria cells were incrustated by silver nanoparticles. The size of the nanoparticles inside the cell ranged from 1 to 40 nm. The size of the silver nanoparticles which were precipitated outside the bacteria cells was in the range

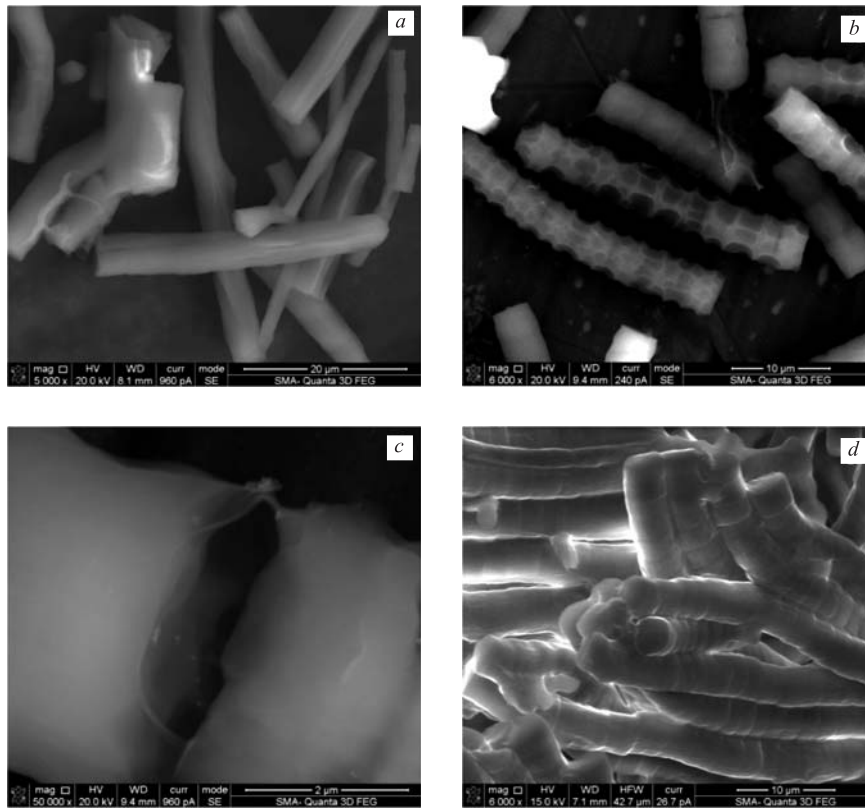


Fig. 11. SEM of *S. platensis* cells: *a*) control; *b, c*) at 1 mM AgNO₃ for 1 day, and *d*) at 1 mM AgNO₃ for 5 days

of 1 to 200 nm. The bioreduction of the Ag⁺ ions was associated with metabolic processes utilizing nitrate by reducing nitrate to nitrite and ammonium.

The silver-resistant bacterial strain *Pseudomonas stutzeri* AG259 isolated from silver mines accumulates silver nanoparticles in the cells where particle size ranges from 35 to 46 nm [29]. Larger particles (200 nm or more) are formed when *P. stutzeri* AG259 is placed in a concentrated aqueous solution of silver nitrate (50 mM).

We assume that the synthesis of silver nanoparticles by *S. platensis* proceeded differently under the short-term and long-term silver action. The exact reaction mechanisms for formation of silver nanoparticles by *S. platensis* should be elucidated. This will help to develop a rational microbial nanoparticle synthesis procedure.

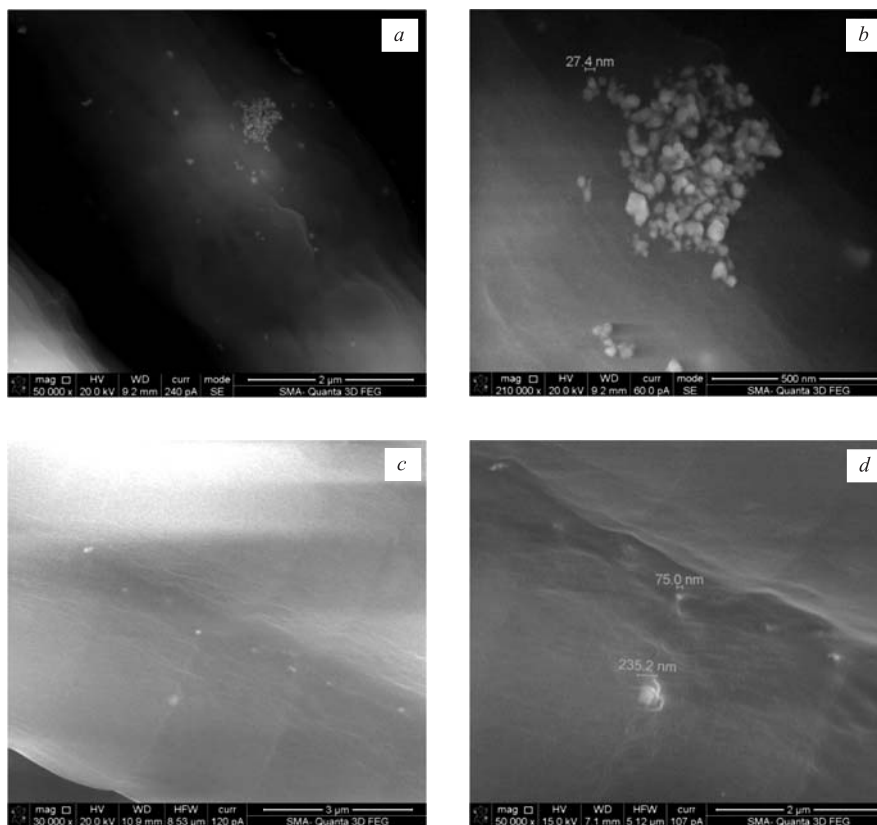


Fig. 12. SEM of *S. platensis* cells at different magnifications: *a, b*) at 1 mM AgNO₃ for 1 day and *c, d*) at 1 mM AgNO₃ for 5 days

CONCLUSIONS

1. The morphological and physiological characterization of the novel actinomycetes strain *Streptomyces glaucus* 71 MD isolated from a soy rhizosphere was conducted in Georgia.

According to our experiments, the tested actinomycetes *Streptomyces glaucus* 71 MD produces silver nanoparticles extracellularly when acted upon by the silver nitrate solution, which offers a great advantage over an intracellular process of synthesis from the point of view of applications.

TEM, SEM, EDAX were used to characterize the silver nanoparticles. TEM showed formation of nanoparticles in the range of 4–25 nm with an average of 13 nm.

2. Production of silver nanoparticles proceeded extracellularly by blue-green microalgae *Spirulina platensis*; however, in this study we have shown that this process depends on the experimental conditions. Specifically, it is different under the short-term and long-term silver action. After 1 day of action by 1 mM AgNO₃, nanoparticles were arranged into long aggregates along *S. platensis* cells strongly damaged by silver ions. However, after 5 days of silver action, *S. platensis* cells were completely recovered and the nanoparticles were distributed more uniformly on the surface of cells (with maximum size of 235 nm and minimum size of 75 nm).

Acknowledgements. This work was financially supported by the Ukrainian Science and Technology Centre (STCU Grant # STCU 4744). We are grateful to Dr. V. Gabunia for helping with the XRD measurements. We acknowledge Dr. E. Ginturi, N. Kuchava and N. Bagdavazde for preparation of samples of *Spirulina platensis*.

REFERENCES

1. Edelstein S., Cammarata R. C. Nanomaterials: Synthesis, Properties and Applications. Institute of Physics Publishing, 1996.
2. Krebig U., Vollner M. Optical Properties of Metal Clusters / Eds. Gonser U., Osgood R.M., Panish M.B., Sakakai H. Berlin: Springer, 1995. P. 207–234.
3. Rai M. et al. // Biotechnol. Adv. 2009. V. 27. P. 76–83.
4. Strosio M.A., Dutta M. Biological Nanostructures and Applications of Nanostructures in Biology: Electrical, Mechanical, and Optical Properties. N.Y. Kluwer Academic Publisher, 2002.
5. Mohanpuria M.P. et al. // J. Nanopart. Res. 2008. V. 10. P. 507–517.
6. Mandal D. et al. // Appl. Microbiol. Biotechnol. 2006. V. 69. P. 485–492.
7. Fortin D., Beveridge T.J. Biomineralization: From Biology to Biotechnology and Medical Applications / Ed. Baeuerien E. Weinheim: Wiley-VCH, 2000.
8. Sharma S. et al. // Mat. Sci. Appl. 2010. V. 1. P. 1–7.
9. Kathirsen K. et al. // Colloid Surface B. 2009. V. 71. P. 133–137.
10. Lengke F.M. et al. // Langmuir. 2007. V. 23. P. 2694–2699.
11. Minaeian S. et al. // Process Biochem. 2007. V. 42. P. 919–923.
12. Sadowski Z. Biosynthesis and Application of Silver and Gold Nanoparticles. Wroclaw University of Technology, 2009. P. 257–276.
13. Govindaraju K. et al. // Geitler. J. Mater. Sci. 2008. V. 43. P. 5115–5122.
14. Mukherjee P. et al. // Nanotechnology. 2008. V. 19. P. 75103; DOI: 10.1088/0957-4484/19/7/075103.
15. Richmond A. Microalgal Biotechnology: Spirulina / Eds. Borowitzka M., Bor J. N.Y.: Cambridge University Press, 1988.
16. Mosulishvili L.M. et al. R. F. Patent 2001106901/14 (007221), 2003.
17. Mosulishvili L.M. et al. R. F. Patent 2002115679/15(016488), 2003.

18. *Sastry M. et al. // Curr. Sci. India. 2003. V. 85. P. 162–170.*
19. *Pataraya D. T. et al. // Annals of Agrarian Science. 2009. V. 7(2). P. 70–74.*
20. *Krassilnikov N. A. Method of Soil Microorganisms and Their Metabolites Study. M.: Publishing House of Moscow University, 1966 (in Russian).*
21. *Pridhem T. C. et al. // J. Bacteriol. 1948. V. 56(1). P. 107–114.*
22. *Egorov N. S. Microbes-Antagonists and the Biological Methods of Determination of Antibiotic Activity. M.: Visshaja Shkola, 1965.*
23. *Petrova I. S. Proteolytical Enzymes of Actinomycetes. M.: Nauka, 1976.*
24. *Krassilnikov N. A. Actinomycetes. M.: Nauka, 1970 (in Russian)*
25. *Bergey's Manual of Determinative Bacteriology / Eds. J.G. Holt, N.R. Krieg, P. H. A. Sneath, J. T. Staley, S. T. Williams. V. 2. M.: Mir, 1997.*
26. *Mosulishvili L. M. et al. // J. Radioanal. Nucl. Ch. 2002. V. 252. P. 15–20.*
27. *Mulvaney P. // Langmuir. 1996. V. 12(3). P. 788–800.*
28. The XRD patterns were indexed with reference to the crystal structures from the ASTM chart card No. 04-0783
29. *T. Klaus et al. // Trends Biotechnol. 2001. V. 19. P. 15–20.*

Received on February 25, 2011.

Корректор *Т. Е. Попеко*

Подписано в печать 6.04.2011.

Формат 60 × 90/16. Бумага офсетная. Печать офсетная.

Усл. печ. л. 1,43. Уч.-изд. л. 1,93. Тираж 260 экз. Заказ № 57303.

Издательский отдел Объединенного института ядерных исследований
141980, г. Дубна, Московская обл., ул. Жолио-Кюри, 6.

E-mail: publish@jinr.ru

www.jinr.ru/publish/